AT&T BELL LABORATORIES TECHNICAL JOURNAL
Vol. 63, No. 4, April 1984
Printed in U.S.A.

Processing Channel-Bank Spectrometer Data

By H. E. ROWE*

(Manuscript received June 29, 1983)

A channel-bank spectrometer produces weighted samples of its input spectrum, the weighting function being determined by the shape of the channel filters. We desire to compare two different input spectra, with similar shape but different widths, from their corresponding weighted samples. This problem arises in millimeter-wave astronomy. For example, a given astronomical source may contain two isotopes of the same molecule. If we know their rest frequencies, comparison of their observed spectra, with appropriate frequency shifts and scale changes, can determine whether the two isotopes have the same velocity distribution. Given the weighted samples for a particular input spectrum, we find the optimum way to calculate the samples for a narrower spectrum having the same shape. We determine the noise and distortion both for this optimum method and for an approximation to it. These results are compared for a particular example with those obtained from an ad-hoc algorithm called "Squish", currently used for this purpose; in this case Squish is almost as good as the approximation to the optimum method. The present results permit such comparisons in other cases that may be of interest, where the present method may offer significant improvement.

I. INTRODUCTION

Consider two well-separated spectral lines observed in a particular radio astronomical source. The intrinsic line widths are usually much smaller than the Doppler spread. If the lines correspond to two isotopes of the same molecule and have the same velocity distribution, these two lines will have the same normalized shape, the higher-frequency line being wider. Let their spectral densities be $P_{s_1}(f)$ and $P_{s_2}(f)$,

* AT&T Bell Laboratories.

centered on frequencies f_1 and f_2, respectively, with $f_2 > f_1$. Since Doppler frequency shift Δf and relative velocity v are related by $\Delta f/f = v/c$, where c is the velocity of light, the line widths are proportional to the ratio of center frequencies

$$\rho \equiv \frac{f_2}{f_1} > 1, \tag{1}$$

and the line shapes are related by

$$P_{s_2}(\rho f) = C \cdot P_{s_1}(f - f_2 + f_1) \tag{2}$$

if the two isotopes have the same velocity distribution, where the "shrink" parameter ρ is given by (1) and C is a line strength parameter. We call $P_{s_2}(\rho f)$ the "shrunk" version of $P_{s_2}(f)$.

The spectral density is not observed directly, but rather measured with a channel-bank spectrometer. This consists of a fixed bank of equally spaced filters of identical shape, each with its own detector. The input spectrum is first translated in frequency so that it lies at the center of the band covered by the filter bank. The detector outputs represent weighted, noisy samples of the input spectral density.

Let the translated spectra of the two isotopes be denoted $\hat{P}_{s_1}(f)$ and $\hat{P}_{s_2}(f)$; their centers now coincide. Then if

$$\hat{P}_{s_2}(\rho f) = C \cdot \hat{P}_{s_1}(f) \tag{3}$$

the two isotopes have the same velocity distribution. We must determine whether this is so by examining the spectral samples, corresponding to $\hat{P}_{s_2}(f)$ and $\hat{P}_{s_1}(f)$, produced by the spectrometer. To do so, we must compute the spectral samples of the shrunk spectrum $\hat{P}_{s_2}(\rho f)$ in terms of the measured spectral samples of the actual input spectrum $\hat{P}_{s_2}(f)$.

We therefore consider the following problem. A spectrometer with input spectral density $P_s(f)$ produces weighted spectral samples x_k, with sample noises n_k. Expressions for x_k and for the statistics of the n_k are given in the next section, and derived in the appendix. Denote the noiseless samples of the shrunk spectrum $P_s(\rho f)$ by $x_{\rho,k}$. Then we wish to estimate the set $\{x_{\rho,k}\}$ from the set $\{x_k + n_k\}$, and determine the mean-square estimation errors due to noise and distortion. This is accomplished by standard linear estimation techniques.

II. CHANNEL-BANK SPECTROMETER ANALYSIS

A typical section of a channel-bank spectrometer is illustrated in Fig. 5 in the appendix. The input signal plus noise are filtered, square-law rectified, and integrated to produce the output spectral sample. Equation (67) gives the spectral sample in terms of the input spectral

density and the common channel filter shape. For convenience, we consider an analogous time-domain model, in which approximate samples of a pulse $x(t)$ are obtained as follows:

$$x_k \equiv \int_{-\infty}^{\infty} x(t)a(t - kT)dt, \qquad -\infty < k < \infty. \tag{4}$$

The spectrum being measured is represented as $x(t)$, and hence is real, positive, and symmetric; the weight function $a(t)$ represents the square magnitude of the baseband equivalent channel-bank filter transfer function (64), and so it is real and positive, but not necessarily symmetric:

$$x(t) = x^*(t) = x(-t) \geqslant 0; \qquad a(t) = a^*(t) \geqslant 0. \tag{5}$$

Denote the Fourier transforms of $x(t)$ and $a(t)$ by $X(f)$ and $A(f)$, respectively. If $x(t)$ is passed through a filter with transfer function $A(-f)$, as in Fig. 1, the x_k are sample values of the filter output. $X(f)$ is real and symmetric (but not necessarily positive), while $A(f)$ is Hermetian. The weight function is normalized to unity at $t = 0$, its nominal center:

$$a(0) = \int_{-\infty}^{\infty} A(f)df = 1. \tag{6}$$

This corresponds to unit gain at midband of the channel-bank filters. A constant input will yield constant samples scaled by $A(0)$, the dc gain of the weighting filter:

$$x(t) = C, \qquad x_k = C \int_{-\infty}^{\infty} a(t)dt = C \cdot A(0). \tag{7}$$

The second-order sample noise statistics for a simultaneous channel-bank spectrometer are given in (76) and (86) when the integration time $\mathcal{T}$ for the integrator in Fig. 5 is large compared to the reciprocal channel-bank filter bandwidth (75). Thus, sample noises n_k are added to each of the samples x_k of (4); the resulting noisy samples are

$$x_k + n_k, \qquad -\infty < k < \infty. \tag{8}$$

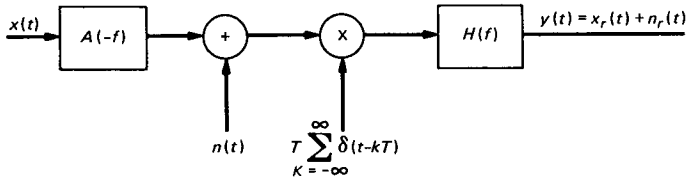

Fig. 1—Model of channel-bank spectrometer.

The n_k have the following statistics:

$$\langle n_k^2 \rangle = N \tag{9}$$

and

$$\langle n_{k+\kappa} n_k \rangle = N\phi_\kappa; \qquad \phi_\kappa = \frac{\int_{-\infty}^{\infty} a(t)a(t + \kappa T)dt}{\int_{-\infty}^{\infty} a^2(t)dt}. \tag{10}$$

The noise power N (77) is directly proportional to receiver noise temperature squared and inversely proportional to integration time. If different channel-bank filters overlap very little, i.e., if the weight functions $a(t - kT)$ for different k in (4) have little overlap, then different noise samples will have small correlation (10).

Finally, we recover an output $y(t)$ by a linear stationary operation on the infinite set of noisy samples (8),

$$y(t) = T \sum_{k=-\infty}^{\infty} (x_k + n_k)h(t - kT). \tag{11}$$

The weight function $h(t)$ chosen for reconstruction depends on what we desire as output.

The above set of operations may be represented by the block diagram of Fig. 1. The pulse $x(t)$ is passed through a filter with transfer function $A(-f)$, where $A(f)$ is the Fourier transform of $a(t)$ of (4):

$$A(f) = \int_{-\infty}^{\infty} a(t)e^{-j2\pi ft}dt. \tag{12}$$

Bandlimited Gaussian noise $n(t)$ is added, with spectral density

$$\begin{aligned} P_n(f) &= NT \sum_{m=-\infty}^{\infty} \phi_m e^{-j2\pi mfT}, \qquad |f| < \frac{1}{2T} \\ P_n(f) &= 0, \qquad |f| > \frac{1}{2T}. \end{aligned} \tag{13}$$

Here ϕ_m is the normalized discrete covariance of the noise samples, given in terms of the channel-bank filter characteristic a of (4) by (9) and (10). If the different filters overlap very little, the noise spectrum of (13) will be almost white. The noisy filtered output is sampled at interval T; finally, a reconstruction filter with transfer function

$$H(f) = \int_{-\infty}^{\infty} h(t)e^{-j2\pi ft}dt \tag{14}$$

yields an output $y(t)$ composed of a signal component $x_r(t)$ and noise

component $n_r(t)$ as shown. From (11) we get:

$$x_r(t) = T \sum_{k=-\infty}^{\infty} x_k h(t - kT)$$
$$n_r(t) = T \sum_{k=-\infty}^{\infty} n_k h(t - kT). \tag{15}$$

Returning to the problem in the introduction, from the noisy samples (8) we wish to estimate

$$x_{\rho,k} = \int_{-\infty}^{\infty} x(\rho t) a(t - kT) dt, \qquad -\infty < k < \infty, \tag{16}$$

with

$$\rho > 1, \tag{17}$$

i.e., the spectrometer response to the shrunk spectrum. In the noiseless case if we require that this be done without error, then we must be able to perfectly reconstruct $x(t)$ from x_k of (4); this requires that $x(t)$ be bandlimited:

$$X(f) = 0, \qquad f > W; \qquad WT < 0.5. \tag{18}$$

There is no aliasing as long as the bandwidth W of $x(t)$ is less than $1/(2T)$, where T is the sampling interval. Since only noise exists outside this band, $|f| > W$, we take the reconstruction filter transfer function to be zero there, whatever its purpose:

$$H(f) = 0, \qquad |f| > W. \tag{19}$$

The output noise $n_r(t)$ of Fig. 1 is stationary, as we see by (13) and (19).

We now determine $H(f)$, $|f| < W$, in order to recover the "shrunk" samples (16) from the noiseless samples (4).

III. DISTORTIONLESS ESTIMATE OF SHRUNK SPECTRUM

Assume that $x(t)$ is bandlimited (18) and that the added noise (9) is zero, $N = 0$. We wish to choose $h(t)$ in (11) such that the samples $x_r(\rho kT)$ of (15) and $x_{\rho,k}$ of (16) are equal:

$$x_r(\rho kT) = x_{\rho,k}. \tag{20}$$

From (18), (19), and Fig. 1 we see that

$$X_r(f) = A(-f)H(f)X(f). \tag{21}$$

For (20) we require

$$X_r\left(\frac{f}{\rho}\right) = A(-f)X\left(\frac{f}{\rho}\right). \tag{22}$$

Comparing (21) and (22) we get

$$H(f) = \begin{cases} \dfrac{A(-\rho f)}{A(-f)}, & |f| < W; \\ 0, & |f| > W; \end{cases} \qquad 0 < WT < 0.5. \tag{23}$$

Equation (23) gives the transfer function for the ideal reconstruction filter for the bandlimited case (18), in the absence of noise. The bandlimited case in our time-domain model corresponds in the appendix to an input spectral density $P_s(f)$ that varies sufficiently slowly compared to the channel-bank filter spacing, F. We will use the filter (23) throughout, and calculate the resulting errors due to noise, and to linear distortion and aliasing when (18) is not satisfied.

The noise $n_r(t)$ in Fig. 1 is stationary; consequently, the noise associated with the samples (20) is

$$\langle n_r^2 \rangle = \int_{-W}^{W} P_n(f) \left| \frac{A(\rho f)}{A(f)} \right|^2 df, \qquad WT < 0.5, \tag{24}$$

where $P_n(f)$ is given by (13). If the noise is almost white, we may set $P_n(f) = NT$.

The reconstruction filter characteristic (23) depends on the shrink factor, ρ. If for a given ρ we desire a fixed filter for all spectra that can be handled by the spectrometer, we take $WT = 0.5$. However, if we know that a given spectrum varies more slowly, we can improve the signal-to-noise ratio by taking a smaller value for W. The minimum value for W, for bandlimited $x(t)$ (18), is determined by our present requirement that the aliasing be zero.

IV. DISTORTION IN ESTIMATE OF SHRUNK SPECTRUM

Suppose now that $x(t)$ is not strictly bandlimited as in (18), but merely that $X(f)$ falls off rapidly for $|f| > 1/(2T)$. Suppose further that we estimate the shrunk spectrum by the reconstruction filter of (23) with $W = 1/(2T)$ (recall that W is no longer the bandwidth of $x(t)$). There will now be linear distortion and aliasing in the estimate. The principal aliasing will come from the first-order modulation products at the sampler output in Fig. 1. Assume that the added noise (9) is zero, $N = 0$. Then (20), (21), and (22) become, respectively:

$$x_r(\rho kT) = x_{\rho,k} + d(\rho kT), \tag{25}$$

$$X_r(f) = X(f)A(-\rho f) + \left[X\left(f - \frac{1}{T}\right) A\left(-f + \frac{1}{T}\right) + X\left(f + \frac{1}{T}\right) A\left(-f - \frac{1}{T}\right)\right] \frac{A(-\rho f)}{A(-f)}, \qquad |f| < \frac{1}{2T}$$

$$X_r(f) = 0, \qquad |f| > \frac{1}{2T}. \tag{26}$$

$$X_r\left(\frac{f}{\rho}\right) = A(-f)X\left(\frac{f}{\rho}\right) + D\left(\frac{f}{\rho}\right). \tag{27}$$

If we compare (26) and (27), the distortion $D(f)$ is given by

$$D(f) = \left[X\left(f - \frac{1}{T}\right) A\left(-f + \frac{1}{T}\right) + X\left(f + \frac{1}{T}\right) A\left(-f - \frac{1}{T}\right)\right] \frac{A(-\rho f)}{A(-f)}, \qquad |f| < \frac{1}{2T}, \tag{28}$$

$$D(f) = -A(-\rho f)X(f), \qquad |f| > \frac{1}{2T}.$$

The inverse transform of (28), $d(t)$, determines the distortion in the reconstructed samples of the shrunk spectrum (25). The noise remains as given by (24).

If $X(f)$ is strictly bandlimited (18) to $|f| < 1/(2T)$, $d(t) = 0$, and we have perfect reconstruction of the shrunk spectrum (Section III) in the absence of noise.

V. SUMMARY OF RESULTS

An input spectrum $x(t)$ is analyzed by a channel-bank spectrometer, producing spectral samples x_k (4) with additive noise samples n_k (8) through (10).

A shrunk spectrum $x(\rho t)$, $1 < \rho$, will similarly produce spectral samples $x_{\rho,k}$, with the same noise samples n_k.

We estimate $x_{\rho,k}$ by $y(\rho kT)$, with $y(t)$ given by (11) with $h(t)$ the inverse transform of (23). Then:

$$y(\rho kT) = x_{\rho,k} + n_r + d(\rho kT). \tag{29}$$

In the absence of noise and distortion, the second and third terms of (29) are zero, and $y(\rho kT)$ gives perfect results for the spectral samples $x_{\rho,k}$ of the shrunk spectrum $x(\rho t)$. Zero distortion requires that $X(f)$ be bandlimited (18), i.e., $X(f) = 0, f > 1/(2T)$.

The noise power $\langle n_r^2 \rangle$ is given by (24).

The distortion $d(t)$ is approximately the inverse Fourier transform of (28). This may be evaluated if we know the input spectrum $x(t)$. However, normally this is what we are trying to measure; it is of course obvious that $d(t)$ cannot be determined merely from the spectral samples x_k, even in the absence of noise. Consequently, (28) is of value only for calculating the distortion in representative cases, not for removing its effects in a given set of measurements.

VI. SINGLE-POLE FILTER

Assume the channel-bank filters are single pole. For this characteristic the above results are readily written out in closed form. Then $a(t)$ of (4) and its Fourier transform $A(f)$ are:

$$a(t) = \frac{1}{1 + \left(\frac{t}{t_o}\right)^2} \tag{30}$$

and

$$A(f) = \pi t_o e^{-2\pi t_o |f|}. \tag{31}$$

The 3-db half-width of the filter is t_o. Assume the spacing between adjacent filters is such that their transfer functions coincide at the 3-db points:

$$T = 2t_o. \tag{32}$$

The noise sample correlation is

$$\phi_m = \frac{1}{1 + m^2}. \tag{33}$$

The power spectrum of the added noise (Fig. 1) is

$$\begin{aligned} P_n(f) &= NT \sum_{m=-\infty}^{\infty} \frac{1}{1 + m^2} e^{-j2\pi mTf}, \qquad |f| < \frac{1}{2T} \\ P_n(f) &= 0, \qquad |f| > \frac{1}{2T}. \end{aligned} \tag{34}$$

The transfer function of the reconstruction filter is (23)

$$\begin{aligned} H(f) &= e^{-\pi T(\rho-1)|f|}, \qquad |f| < \frac{1}{2T} \\ H(f) &= 0, \qquad |f| > \frac{1}{2T}. \end{aligned} \tag{35}$$

The impulse response of the reconstruction filter is

$$h(t) = 2\,\frac{\pi T(\rho - 1)\left[1 - e^{-\frac{\pi}{2}(\rho-1)} \cos \pi \frac{t}{T}\right] + 2\pi t e^{-\frac{\pi}{2}(\rho-1)} \sin \pi \frac{t}{T}}{[\pi T(\rho - 1)]^2 + (2\pi t)^2}. \tag{36}$$

Observe that as $\rho \to 1$, $h(t) \to [\sin \pi(t/T)]/(\pi t)$.

The Fourier transform of the distortion $d(t)$ is (28):

$$D(f) = \frac{\pi T}{2} e^{-\pi} e^{\pi\rho Tf} \left[X\left(f - \frac{1}{T}\right) + X\left(f + \frac{1}{T}\right) e^{-2\pi Tf} \right], \qquad -\frac{1}{2T} < f < 0$$

$$D(f) = \frac{\pi T}{2} e^{-\pi} e^{-\pi\rho Tf} \left[X\left(f - \frac{1}{T}\right) e^{2\pi Tf} + X\left(f + \frac{1}{T}\right) \right], \qquad 0 < f < \frac{1}{2T} \tag{37}$$

$$D(f) = -\frac{\pi T}{2} e^{-\pi\rho T|f|} X(f), \qquad |f| > \frac{1}{2T}.$$

For $x(t)$ essentially bandlimited, $X(f)$ will fall off rapidly for $|f| > 1/(2T)$, and most of the contribution to $D(f)$ occurs for $|f|$ near $1/(2T)$. In this region we may approximate $D(f)$ by exponentials.

Finally, the output sample noise is

$$\langle n_r^2 \rangle = \frac{N(\rho - 1)}{\pi} \sum_{m=-\infty}^{\infty} \frac{1}{1 + m^2} \frac{1 - (-1)^m e^{-\pi(\rho-1)}}{(\rho - 1)^2 + m^2}$$

$$= \frac{N}{\rho} \left[1 + 2 \frac{\rho - 1}{2 - \rho} \frac{e^{-\pi\rho} - e^{-2\pi}}{1 - e^{-2\pi}} \right]. \tag{38}$$

Suppose we approximate $P_n(f)$ of (34) by its $m = 0$ term, i.e., regard $P_n(f)$ as white or equivalently neglect correlation between different noise samples (10). This corresponds to keeping only the $m = 0$ term in the output sample noise, in the first line of (38):

$$\langle n_r^2 \rangle \approx \frac{N}{\pi(\rho - 1)} [1 - e^{-\pi(\rho-1)}], \qquad P_n(f) \text{ white.} \tag{39}$$

As $\rho \to 1$ (39) and (38) both yield $\langle n_r^2 \rangle \to N$. This suggests that for expansion factors only a little larger than unity, the correlation between noise samples may be neglected.

The single-pole filter is special in that most of the general results may be written out explicitly. In contrast, approximations are used in the treatment of more general filters, such as the double-pole filter treated in the following section.

VII. DOUBLE-POLE FILTER

We now consider maximally flat double-pole channel-bank filters. $a(t)$ of (4) and its Fourier transform $A(f)$ are:

$$a(t) = \frac{1}{1 + \left(\frac{t}{t_o}\right)^4} . \tag{40}$$

$$A(f) = \frac{\pi t_o}{\sqrt{2}} e^{-\sqrt{2}\pi t_o |f|} \left[\cos\sqrt{2}\pi t_o f + \sin\sqrt{2}\pi t_o |f|\right] . \tag{41}$$

t_o is the 3-db half-width of the filter. We again assume that the spacing between adjacent filters is such that their transfer functions coincide at the 3-db points:

$$T = 2t_o. \tag{42}$$

The calculation of ϕ_m of (10) is straightforward but messy. Rather than perform it here, we rely on the example of the single-pole filter, treated in the preceding section, which suggests that correlation between noise samples is unimportant. Consequently, we take $\phi_m \approx 0$, $m \neq 0$, thus approximating the noise of (13) and Fig. 1 as white; note that $\phi_0 = 1$.

The transfer function $H(f)$ of the reconstruction filter is determined by substituting (41) into (23). Unlike the single-pole filter of the preceding section, in the present case the inverse transform, yielding the reconstruction filter impulse response $h(t)$, is not readily calculated exactly. Consequently, we must either invert $H(f)$ numerically for each value of ρ, or use an approximation valid for ρ in the range of interest, here a little larger than one.

First, we note that since $|f| < 1/(2T)$, the maximum value of the argument (in exponential and trigonometric functions) that can occur in (41) and (42) is $\pi/(2\sqrt{2}) \approx 1.111$. Next, the first zero of (41) and (42) occurs when the argument is $3\pi/4 \approx 2.356$. Consequently, a zero of (41) and (42) never occurs in the range of interest, and consequently $H(f)$ of (23) will never have a pole.

$H(f)$ decreases monotonically as f varies from 0 to $1/(2T)$, and remains positive for $0 < \rho < 2$. This suggests a parabolic approximation:

$$H(f) \begin{cases} \approx 1 - K_\rho(2Tf)^2, & |f| < \dfrac{1}{2T} \\ = 0, & |f| > \dfrac{1}{2T} . \end{cases} \tag{43}$$

For Taylor series approximation $K_\rho = (\pi^2/8)(\rho^2 - 1)$. Alternatively, we may approximate $H(f)$ by a parabola that agrees exactly at $f = 0$

and $f = \pm 1/(2T)$. For $\rho = 1.05$ the agreement is better than 0.3 percent, while for $\rho = 1.1$ the agreement is better than 0.75 percent. For this approximation

$$K_\rho = 1 - \frac{e^{-\frac{\pi}{2\sqrt{2}}\rho}\left(\cos\frac{\pi}{2\sqrt{2}}\rho + \sin\frac{\pi}{2\sqrt{2}}\rho\right)}{e^{-\frac{\pi}{2\sqrt{2}}}\left(\cos\frac{\pi}{2\sqrt{2}} + \sin\frac{\pi}{2\sqrt{2}}\right)}. \tag{44}$$

The corresponding filter impulse response is in either case

$$h(t) = \frac{1}{T}\frac{\sin\frac{\pi t}{T}}{\frac{\pi t}{T}} + \frac{K_\rho}{T}\frac{2\frac{\pi t}{T}\sin\frac{\pi t}{T} - \left(\frac{\pi t}{T}\right)^3\sin\frac{\pi t}{T} - 2\left(\frac{\pi t}{T}\right)^2\cos\frac{\pi t}{T}}{\left(\frac{\pi t}{T}\right)^4}. \tag{45}$$

The distortion transform $D(f)$ for the ideal case is again given by substituting (41) and (42) into (28). A similar expression is readily written out for the approximate transfer function (43), which yields additional distortion.

The output sample noise, neglecting correlation between noise samples as discussed in the paragraph following (42), with the approximate transfer function of (43), is

$$\langle n_r^2 \rangle \approx N(1 - K_\rho). \tag{46}$$

VIII. EXAMPLE: DOUBLE-POLE FILTER, LORENTZ SPECTRUM

Assume a Lorentz spectrum as input:

$$x(t) = \frac{1}{1 + \left(\frac{t}{t_\mathscr{L}}\right)^2}. \tag{47}$$

Assume the channel-bank filter characteristic is given by (40), with separation given by (42). The samples x_k (4) are

$$x_k = \frac{\pi T}{2\sqrt{2}}\frac{\left(\frac{T}{t_\mathscr{L}}k\right)^2 + \left(1 + \frac{T}{\sqrt{2}t_\mathscr{L}}\right)\left[1 + \frac{T}{\sqrt{2}t_\mathscr{L}} + \left(\frac{T}{2t_\mathscr{L}}\right)^2\right]}{\left(\frac{T}{t_\mathscr{L}}k\right)^4 + 2\left(1 + \frac{T}{\sqrt{2}t_\mathscr{L}}\right)\left(\frac{T}{t_\mathscr{L}}k\right)^2 + \left[1 + \frac{T}{\sqrt{2}t_\mathscr{L}} + \left(\frac{T}{2t_\mathscr{L}}\right)^2\right]^2}. \tag{48}$$

For line width large compared to the filter spacing, $t_{\mathscr{L}} \gg T$,

$$\frac{T}{t_{\mathscr{L}}} \xrightarrow{\lim} 0 \; x_k = \frac{\pi T}{2\sqrt{2}} \frac{1}{1 + \left(\frac{T}{t_{\mathscr{L}}} k\right)^2}. \tag{49}$$

The samples $x_{\rho,k}$ (16) are found by substituting $t_{\mathscr{L}} \to t_{\mathscr{L}}/\rho$ in (48).

The transform $D(f)$ of the distortion $d(t)$ of (25) is given as follows:

$$\begin{aligned} D(f) &= A(-\rho f)X(f)\left[\frac{A(-f)}{A(-\rho f)} H(f) - 1\right] \\ &\quad + \left[X\left(f - \frac{1}{T}\right) A\left(-f + \frac{1}{T}\right)\right. \\ &\quad \left. + X\left(f + \frac{1}{T}\right) A\left(-f - \frac{1}{T}\right)\right] \cdot H(f), \qquad |f| < \frac{1}{2T}. \\ D(f) &= -A(-\rho f)X(f), \qquad |f| > \frac{1}{2T}. \end{aligned} \tag{50}$$

Here $A(f)$ is given by (41) and (42), and $X(f)$ is the transform of (47):

$$X(f) = \pi t_{\mathscr{L}} e^{-2\pi t_{\mathscr{L}} |f|}. \tag{51}$$

For $H(f)$ the ideal reconstruction filter of (23), (41) and (42), and (50) yields (28). The approximate $H(f)$ of (43) yields additional distortion. Various approximations are necessary in different cases to evaluate $d(t)$ as the inverse transform of (50).

As a single illustration, assume a Lorentz spectrum with half-width equal to five times the filter spacing:

$$\frac{t_{\mathscr{L}}}{T} = 5. \tag{52}$$

Assume a shrink factor

$$\rho = 1.1. \tag{53}$$

Figure 2 shows the transform of the desired output; Fig. 3 shows the transform of the distortion with the ideal reconstruction filter (23), (41), and (42); and Fig. 4 shows the transform of the distortion with the Taylor series approximate filter of (43) with $K_\pi = \pi^2/8\ (\rho^2 - 1)$. Note that the transforms in Figs. 2, 3, and 4 are normalized to $1/(\pi T)^2$.

For the ideal reconstruction filter, the principal contribution to distortion occurs near $|f| = 1/(2T)$. The form of $D(f)$ in Fig. 3 in this region suggests that we approximate $D(f)$ by exponentials; this yields

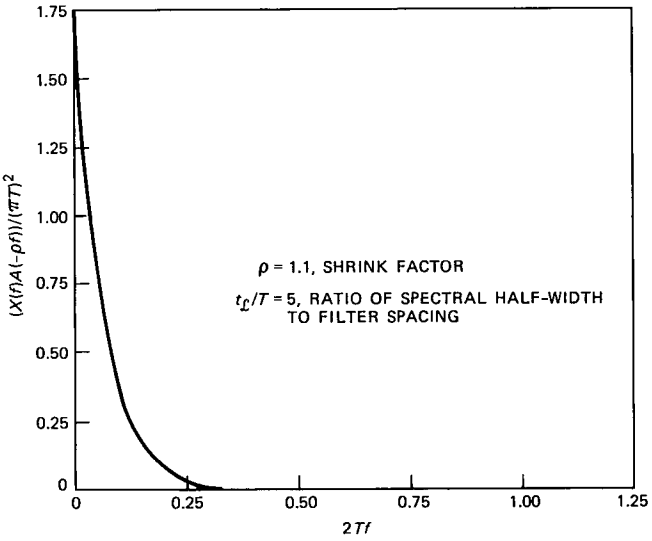

Fig. 2—Desired output for the Lorentz spectrum.

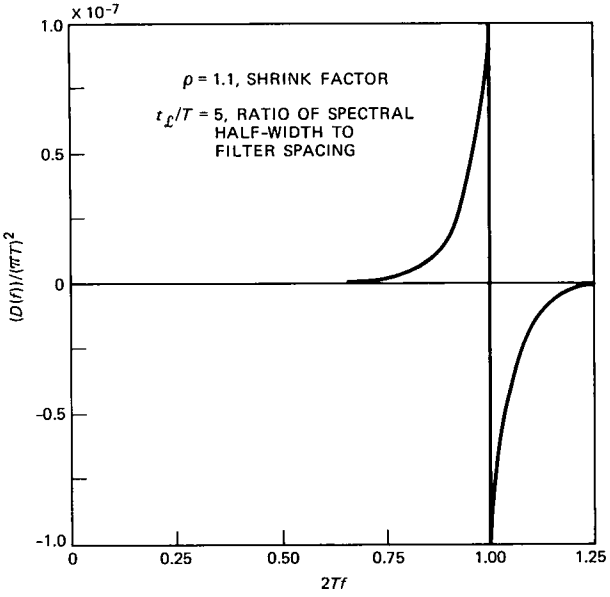

Fig. 3—Distortion with ideal filter for the Lorentz spectrum.

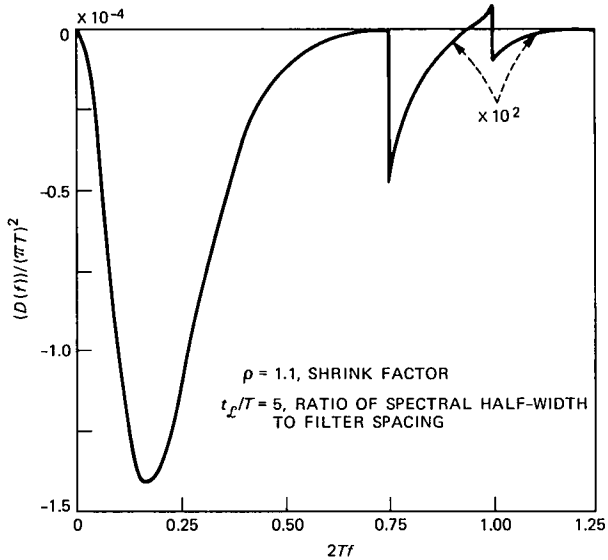

Fig. 4—Distortion with Taylor series filter for the Lorentz spectrum.

a closed-form approximation for $d(t)$, and thence for the error $d(\rho kT)$ in the reconstructed samples (29). Similarly, for the Taylor series approximate filter the form of $D(f)$ in Fig. 4 suggests a Gaussian approximation for $D(f)$, similar to that used in LaPlace's method, to obtain an approximation for $d(t)$.

We shall not carry out either of these approximations here; rather, we will content ourselves with simple upper bounds on the maximum distortion. Clearly,

$$d_{\max} \equiv d(t)|_{\max} \leq \int_{-\infty}^{\infty} |D(f)|\, df. \tag{54}$$

For the ideal filter, we estimate from Fig. 3 that

$$d_{\max} < \approx 5 \times 10^{-8}\ (\pi^2/2)T \approx 2.5 \times 10^{-7}\ T.$$

This estimate will be too large; $|d(t)|_{\max}$ will occur for t away from the origin, and consequently the maximum error will occur at the edge of the spectrum in (29).

For the Taylor series approximate filter, we estimate from Fig. 4 that $d_{\max} < \approx 1.5 \times 10^{-4}\ (\pi^2/2)\ T \approx 7.5 \times 10^{-4}\ T$. This estimate will be fairly accurate; $d(t)|_{\max}$ occurs for $t = 0$, and consequently the maximum error occurs at the center of the spectrum, $k = 0$ in (29).

Finally, the noise in the reconstructed samples is given approxi-

mately for the Taylor series filter by (46) as

$$\langle n_r^2 \rangle \approx N\left[1 - \frac{\pi^2}{8}(\rho^2 - 1)\right] = 0.741N. \tag{55}$$

The noise for the ideal filter will be a little larger.

IX. "SQUISH"

We compute the distortion and noise in the current algorithm "Squish", for comparison with the results of the preceding section. Squish may be described as follows. Associate with the samples x_k of (4) the function

$$s(t) \equiv \sum_{k=-\infty}^{\infty} x_k \operatorname{rect}\left(\frac{t}{T} - k\right), \tag{56}$$

where we recall that

$$\operatorname{rect}(t) \equiv \begin{matrix} 1, & |t| < 1/2 \\ 0, & |t| > 1/2. \end{matrix} \tag{57}$$

Similarly, define

$$s_q(t) \equiv \sum_{k=-\infty}^{\infty} q_k \operatorname{rect}\left(\frac{t}{\rho T} - k\right). \tag{58}$$

Choose the $\{q_k\}$ such that

$$\int_{t - k\rho T - \frac{\rho T}{2}}^{t - k\rho T + \frac{\rho T}{2}} [s_q(t) - s(t)]dt = 0; \tag{59}$$

equivalently,

$$q_k = \frac{1}{\rho T} \int_{t - k\rho T - \frac{\rho T}{2}}^{t - k\rho T + \frac{\rho T}{2}} s(t)dt. \tag{60}$$

The q_k are assumed to approximate the samples $x_{\rho,k}$ of (16):

$$q_k = x_{\rho,k} + d_k + n_k, \tag{61}$$

where d_k and n_k represent the distortion and noise from the desired output.

The following results correspond to the parameters of (52) and (53).

k	d_k	$\langle n_k^2 \rangle$
0	$-1.85 \times 10^{-3}\ T$	$0.83\ N$
1	$-4.87 \times 10^{-3}\ T$	$0.76\ N$
2	$-4.47 \times 10^{-3}\ T$	$0.65\ N$
3	$-1.59 \times 10^{-3}\ T$	$0.57\ N$
4	$0.91 \times 10^{-3}\ T$	$0.52\ N$
5	$2.18 \times 10^{-3}\ T$	$0.5\ N$
6	$2.51 \times 10^{-3}\ T$	$0.52\ N$
7	$2.36 \times 10^{-3}\ T$	$0.57\ N$
8	$2.02 \times 10^{-3}\ T$	$0.65\ N$
9	$1.65 \times 10^{-3}\ T$	$0.76\ N$
10	$0.12 \times 10^{-3}\ T$	$0.83\ N$

(62)

The peak distortion $d_{\max} \equiv |d_k|_{\max} = 4.87 \times 10^{-3}\ T$ occurs at $k = 1$. The peak noise $\langle n_k^2 \rangle_{\max} = 0.83\ N$ occurs at $k = 0, 10, \cdots$, i.e., when $\rho k =$ integer; the variation of noise with k makes evident the nonstationary nature of "Squish".

X. DISCUSSION

We have shown how to relate the measurements obtained with a channel-bank spectrometer on two spectra, $P_s(f)$ and $P_s(\rho f)$, having similar shape but different scales along the frequency axis. This problem arises in radio astronomy, in determining whether two isotopes have the same velocity distribution.

As a single numerical example, we have considered a Lorentz line 10 samples wide between its half-power points, analyzed by a channel-bank spectrometer with double-pole filters spaced so that their 3-db points coincide. We have determined the noise and distortion in computing the corresponding samples for a Lorentz spectrum 90.9 percent as wide, by the present methods and with the current algorithm "Squish". We summarize these results of Sections VIII and IX in Table I.

Table I—Comparison between present and proposed processing methods

	Ideal Filter	Taylor Series Filter	Squish
Maximum distortion	$<2.5 \times 10^{-7}$ T	7.5×10^{-4} T	4.87×10^{-3} T
Maximum noise power	>0.741 N	0.741 N	0.83 N

These values are to be compared with the maximum sample value, $x_0 = 1.10\ T$, obtained from (48) with $k = 0$.

In the present example Squish has a little more distortion and noise

than the Taylor series approximation to the ideal reconstruction filter; the ideal filter, of course, has much less distortion. For a narrower input spectrum, i.e., larger ρ, Squish will be relatively worse.

Such comparisons may vary widely, depending on the spectrum under study and the channel-bank filter characteristic. The behavior in the main part of the spectrum may be quite different from that far out on the tails.

XI. ACKNOWLEDGMENT

I would like to thank R. W. Wilson for suggesting this problem, and the unknown reviewer for a number of helpful suggestions.

APPENDIX

Output Statistics of Channel-Bank Spectrometer

Figure 5 shows a typical section of a channel-bank spectrometer, consisting of a filter, square-law detector, and integrator. The input $s(t)$ represents the noise whose spectral density $P_s(f)$ we wish to determine; $P_s(f)$ is real and symmetric, i.e., $P_s(f) = P_s^*(f) = P_s(-f)$. $v(t)$ represents the receiver input noise, assumed white, with spectral density $\mathcal{N}$. Assume throughout this appendix that the measurement starts at $t = 0$ and that the integration time is $\mathcal{T}$; then the integrator output $w_k(\mathcal{T})$ is the noisy sample of (8).

We assume the receiver input noise is much larger than the noise whose spectrum is being measured:

$$P_s(f) \ll \mathcal{N}. \tag{63}$$

The random "signal" $s(t)$ and noise $v(t)$ each produce a dc and a random component at the outputs $w_k(t)$. The dc component of $w_k(\mathcal{T})$ due to $s(t)$ is the desired spectral sample. The dc component due to receiver front-end noise $v(t)$ is uninteresting here. The random component due to $s(t)$ is much smaller than the random component due to $v(t)$; we ignore the former, and consider the latter as the "noise" in the sample. In summary, the dc component of $w_k(\mathcal{T})$ due to $s(t)$ (the

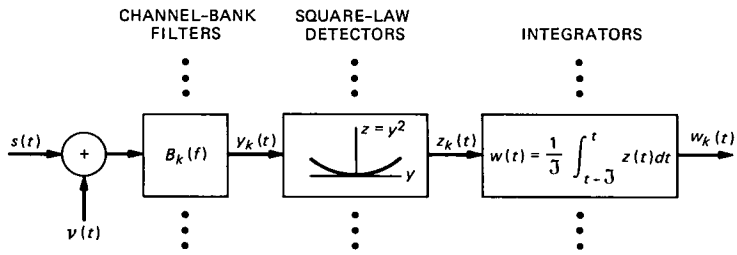

Fig. 5—Typical section of a channel-bank spectrometer.

noise being measured) corresponds to x_k of (4) and (8); the random component due to receiver noise $\nu(t)$ corresponds to n_k of (8) and (9).

Assume the channel-bank filters are equally spaced with the same shape; let $B(f)$ be their common baseband equivalent filter. Then the kth channel-bank filter has transfer function

$$B_k(f) = B(f - kF) + B^*(-f - kF), \tag{64}$$

where F represents the filter spacing. We assume that $B(f)$, and hence $B_k(f)$, are causal; thus their respective Fourier transforms satisfy $b(t) = 0$ and $b_k(t) = 0$ for $t < 0$. $b_k(t)$ is real, but $b(t)$ is not necessarily real; while $B_k(f)$ is Hermetian, $B(f)$ need not be. We also assume that the spectra of interest are narrowband, so that the $\{k\}$ of interest in (64) are large enough such that

$$B(f) \approx 0, \qquad |f| > |k|F, \tag{65}$$

and the two terms in (64) are essentially nonoverlapping.

Assume that $\nu(t) = 0$ in Fig. 5. Then

$$\langle w_k(t)\rangle = \langle z_k(t)\rangle = \langle y_k^2(t)\rangle = \int_{-\infty}^{\infty} |B_k(f)|^2 P_s(f)df. \tag{66}$$

From (64) and (65), we have in terms of the equivalent baseband filter transfer function

$$\langle w_k(\mathscr{T})\rangle = \int_{-\infty}^{\infty} 2|B(f - kF)|^2 P_s(f)df \tag{67}$$

for the desired sample output. Since k and F are positive, by (65) the main contribution to the integral in (67) occurs close to $f \sim kF$, and there is no significant contribution to this integral for $f < 0$. Setting $f \to t$, $F \to T$, $P_s(\,) \to x(\,)$, $2|B(\,)|^2 \to a(\,)$, and $\langle w_k(\mathscr{T})\rangle \to x_k$, we obtain (4).

Assume now that $s(t) = 0$ in Fig. 5. Then

$$\begin{aligned}\langle w_k(t)\rangle = \langle z_k(t)\rangle = \langle y_k^2(t)\rangle &= \mathscr{N}\int_{-\infty}^{\infty} |B_k(f)|^2 df \\ &= \mathscr{N}\int_{-\infty}^{\infty} 2|B(f)|^2 df,\end{aligned} \tag{68}$$

the last step following from (64) and (65). Define

$$\begin{aligned} w_{kac}(t) &\equiv w_k(t) - \langle w_k(t)\rangle \\ z_{kac}(t) &\equiv z_k(t) - \langle z_k(t)\rangle. \end{aligned} \tag{69}$$

Then the spectral density of the second quantity in (69) is

$$P_{z_{kac}}(f) = 2\mathscr{N}^2 |B_k(f)|^2 \circledast |B_k(f)|^2, \tag{70}$$

where $\circledast$ represents convolution. Now the integrator has impulse response

$$i(t) = \begin{cases} \dfrac{1}{\mathcal{T}}, & 0 < t < \mathcal{T} \\ 0, & \text{otherwise.} \end{cases} \tag{71}$$

The integrator transfer function, the Fourier transform of (71), is

$$I(f) = e^{-j\pi f \mathcal{T}} \frac{\sin \pi f \mathcal{T}}{\pi f \mathcal{T}}. \tag{72}$$

Then

$$\langle w_{kac}^2(t) \rangle = \int_{-\infty}^{\infty} |I(f)|^2 P_{z_{kac}}(f) df. \tag{73}$$

Now by (64), $P_{z_{kac}}(f)$ of (70) consists of a low-frequency part centered around $f = 0$,

$$P_{z_{kac}}^{\text{low}}(f) = 4\mathcal{N}^2 |B(f)|^2 \circledast |B(-f)|^2, \tag{74}$$

and a high-frequency part centered around $f = \pm 2kF$. By (65) these two parts are essentially nonoverlapping. Since $|I(f)|^2$ becomes small for $|f| \gg 1/\mathcal{T}$, only the portion (74) will be significant in (73) if $1/\mathcal{T} \ll |k|F$, i.e., if the integration time is large compared to the reciprocal frequency being measured. This is always true, and hence we may replace $P_{z_{kac}}(f)$ in (73) by (74). Moreover, we assume

$$\frac{1}{\mathcal{T}} \ll \text{width of } B(f). \tag{75}$$

Then (73) and (74) yield

$$\langle w_{kac}^2(t) \rangle = \frac{\mathcal{N}^2}{\mathcal{T}} \int_{-\infty}^{\infty} [2|B(f)|^2]^2 df. \tag{76}$$

Setting $f \to t$, $2|B(\,)|^2 \to a(\,)$, and $\langle w_{kac}^2(\mathcal{T}) \rangle \to N$, (76) becomes

$$N = \frac{\mathcal{N}^2}{\mathcal{T}} \int_{-\infty}^{\infty} a^2(t) dt \tag{77}$$

to be substituted in (9) and (10).

Finally, we find the correlation between different noise samples (10); i.e., in the notation of the present appendix we seek

$$\langle w_{kac}(\mathcal{T}).\ w_{k'ac}(\mathcal{T}) \rangle.$$

We set $s(t) = 0$, and have the following relations between cross-spectra:

$$P_{y_k y_{k'}}(f) = \mathcal{N} B_k(f) B_{k'}^*(f). \tag{78}$$

$$P_{w_{kac} w_{k'ac}}(f) = P_{z_{kac} z_{k'ac}}(f) \cdot \left(\frac{\sin \pi f \mathcal{T}}{\pi f \mathcal{T}} \right)^2. \tag{79}$$

We relate $P_{z_{kac} z_{k'ac}}(f)$ to $P_{y_k y_{k'}}(f)$ as follows:

$$\phi_{z_{kac} z_{k'ac}}(\tau) \equiv \langle z_{kac}(t + \tau) z_{k'ac}(t) \rangle$$
$$\equiv \langle y_{kac}^2(t + \tau) y_{k'ac}^2(t) \rangle - \langle z(t) \rangle^2, \tag{80}$$

where we omit the subscript from the final term because the expected detector outputs are the same for all channels by (68). Assuming the receiver input noise $\nu(t)$ is Gaussian, the $y_k(t)$ are jointly Gaussian, and using (68)

$$\phi_{z_{kac} z_{k'ac}}(\tau) = 2\phi_{y_k y_{k'}}^2(\tau). \tag{81}$$

The Fourier transform of (81) yields the following relationship between the cross-spectra of different y and the ac components of corresponding z:

$$P_{z_{kac} z_{k'ac}}(f) = 2 P_{y_k y_{k'}}(f) \circledast P_{y_k y_{k'}}(f). \tag{82}$$

Combining (78), (79), and (82) we get:

$$P_{w_{kac} w_{k'ac}}(f) = 2\mathcal{N}^2 \left[\frac{\sin \pi f \mathcal{T}}{\pi f \mathcal{T}} \right]^2 \cdot [B_k(f) B_{k'}^*(f)] \circledast [B_k(f) B_{k'}^*(f)]. \tag{83}$$

Then

$$\langle w_{kac}(t) w_{k'ac}(t) \rangle = \int_{-\infty}^{\infty} P_{w_{kac} w_{k'ac}}(f) df. \tag{84}$$

By (75) we may approximate $P_{w_{kac} w_{k'ac}}(f)$ of (83) by its value for $f = 0$ in (84), yielding

$$\langle w_{kac}(t) w_{k'ac}(t) \rangle = \frac{2\mathcal{N}^2}{\mathcal{T}} \int_{-\infty}^{\infty} |B_k(f)|^2 |B_{k'}(f)|^2 df. \tag{85}$$

From (64) and (65) we express (85) in terms of the baseband equivalent filter as

$$\langle w_{kac}(t) w_{k'ac}(t) \rangle = \frac{\mathcal{N}^2}{\mathcal{T}} \int_{-\infty}^{\infty} 2|B(f)|^2 \cdot 2|B(f - (k - k')F)|^2 df. \tag{86}$$

Setting $f \to t$, $F \to T$, $2|B(\,)|^2 \to a(\,)$, $\langle w_{kac}(\,\mathcal{T}) w_{k'ac}(\,\mathcal{T}) \rangle \to \langle n_k n_{k'} \rangle$, and $k' - k = \kappa$ in (86), and using (77), we obtain (10).

AUTHOR

Harrison E. Rowe, B.S., M.S., Sc.D. (Electrical Engineering), Massachusetts Institute of Technology, 1948, 1950, and 1952; U. S. Navy, 1945–1946, AT&T

Bell Laboratories, 1952—. Mr. Rowe joined AT&T Bell Laboratories as a Member of Technical Staff in the Radio Research Laboratory. Presently, he is in the Radio Physics Research Department. His publications include numerous papers and one textbook, spanning a variety of fields including parametric amplifiers, noise, and communication theory; propagation in random media; and related problems in waveguide, radio, and optical communication systems. His is the joint author of five patents. Fellow, IEEE; corecipient, 1977 David Sarnoff Award and 1972 Microwave Prize; member, Commission C of URSI, Sigma Xi, Tau Beta Pi, and Eta Kappa Nu.